Neutron Star Astrophysics at the Crossroads: Magnetars and the Multimessenger Revolution
Proceedings IAU Symposium No. 363, 2023
E. Troja & M. G. Baring, eds.
doi:10.1017/S1743921322001193

Magnetorotational core-collapse supernovae: the impact of the magnetic field's structure

Matteo Bugli[1], **Jérôme Guilet**[1] **and Martin Obergaulinger**[2]

[1]Laboratoire AIM, CEA/DRF-CNRS-Université Paris Diderot, IRFU/Département d'Astrophysique, CEA-Saclay, F-91191, Gif-sur-Yvette, France
email: matteo.bugli@cea.fr

[2]Departament d'Astronomia i Astrofísica, Universitat de València, Dr. Moliner 50, 46100, Burjassot, Spain
email: martin.obergaulinger@uv.es

Abstract. The combination of strong magnetic fields and fast rotation is often invoked as a characteristic of the central engine for outstanding sources such as GRBs, hypernovae, and superluminous supernovae. However, the actual properties of the magnetic field during the collapse of the stellar progenitor are very uncertain, since they depend on the evolution of the star and can be affected by complex dynamo processes occurring in the central proto-neutron star. Using 3D relativistic MHD models we show that higher-order multipolar fields can lead to the onset of a supernova, although they tend to produce less energetic explosions and less collimated outflows. Quadrupolar fields efficiently extract angular momentum from the central core, but the rotational energy is partly stored in the equatorial regions, rather than powering up the polar outflows. Finally, our results show a strong magnetic quenching of the hydrodynamic non-axisymmetric instabilities that are associated to the emission of GWs.

Keywords. supernovae: general, stars: neutron, magnetohydrodynamics, MHD, shock waves, instabilities, gravitational waves;

1. Introduction

The vast majority of core-collapse supernovae (CCSN) simulations concern stellar progenitors with modest to no rotation and dynamically neglibible magnetic fields. The onset of their explosion relies on the so-called *neutrino-driven mechanism*, where a small fraction of the energy carried away by neutrinos is deposited behind the shock-wave, leading to its outward expansion across the layers of the progenitor. However, such process cannot explain outstanding stellar explosions such as *hypernovae* (Drout *et al.* 2011), whose ejecta are typically 10 times more energetic than a standard CCSN, and *superluminous supernovae* (Nicholl *et al.* 2017), whose integrated luminosities exceed up to a factor 100 the typical value of 10^{49} erg. The combination of strong large-scale magnetic fields and fast rotation provides a very efficient way to power up such energetic transient, as the rotational energy reservoir can be tapped into by magnetic stresses slowing down the central proto-neutron star (PNS) and launching powerful polar outflows.

In the last 15 years there has been a significant improvement in the quality and sophistication of numerical models of magnetized CCSN (Kuroda *et al.* 2020; Obergaulinger & Aloy 2021), which typically consider a strong aligned dipolar magnetic field ($\sim 10^{12}$ G) as initial condition at the beginning of the gravitational collapse. However, the origin of such magnetic field strength remains a long standing problem.

© The Author(s), 2023. Published by Cambridge University Press on behalf of International Astronomical Union.

https://doi.org/10.1017/S1743921322001193 Published online by Cambridge University Press

A possible solution are in-situ dynamos within the forming PNS that can amplify the magnetic fields through the action of convection (Raynaud *et al.* 2020, 2022) and the magnetorotational instability (MRI, Reboul-Salze *et al.* 2021, 2022). Contrary to what is usually assumed in the aforementioned numerical studies, the resulting magnetic fields are invariably characterized by a complex topology (such as higher multipolar orders and strong non-axisymmetric features). As shown in Bugli *et al.* (2020), performing axisymmetric CCSN simulations with magnetic fields distributed on smaller angular scales (but keeping the same total magnetic energy content) tends to produce weaker explosions, along with more massive and faster rotating PNS. We present here a series of 3D simulations of magnetized CCSN from Bugli *et al.* (2021) that for the first time consider magnetic configurations such as aligned quadrupole or equatorial dipole, comparing them to the hydrodynamic and standard aligned dipole cases.

2. Numerical models

All our models follow the collapse of the 35OC stellar progenitor from Woosley & Heger (2007) with its original rotation profile but employing an ad-hoc magnetic field configuration. Labels H, L1-0, L2-0A and L1-90 refer respectively to the hydrodynamic, aligned dipole, aligned quadrupole and equatorial dipole configurations. The details of the setup, along with the specifics of the code we used to perform our simulations, can be found in Bugli *et al.* (2021).

3. Discussion

While all our models lead to a successful explosion, the morphology and dynamics of the ejecta are quite different. From Fig. 1 we can see how the hydrodynamic benchmark (top left panel) produces a rather spherical distribution of the ejecta that expand at the slowest pace compared to the other models, whereas at the other end model L1-0 (top right) forms two symmetric and well collimated polar outflows. The ejecta of model L2-0A are also distributed preferentially along the rotational axis (although they are expanding more slowly and are less collimated), while the simulation with the equatorial dipole shows a spherical distribution in the external layers closer to the shock wave engulfing higher entropy material distributed vertically. Although our magnetized models develop some large-scale non axisymmetric features, in none of them the structure of the outflow seems to be disrupted by the development of the kink instability (Mösta *et al.* 2014).

The rate at which the ejecta expand correlates directly with the total energy $E_{\rm exp}$ stored in the gravitationally unbound material shown in the left panel of Fig. 2. At the two extremes we have models L1-0 and H, displaying respectively the most and least energetic explosions in our study. The simulation with a quadrupolar field produces instead the second most energetic ejecta, hinting at a plateau in $E_{\rm exp}$ at around $t \simeq 500$ ms p.b. Finally, the explosion energy of model L1-90 grows even slower, reaching also a maximum around the same time and actually decreasing afterwards. If we look at the total angular momentum of the central PNS (right panel) we note that the most energetic explosion in not associated to the slowest PNS, which is instead produced by model L2-0A. This apparent discrepancy is due to the fact that an aligned magnetic dipole transports angular momentum preferentially across the polar regions, where it directly affects the dynamic of the outflow. On the other hand, a quadrupolar field (or an equatorial dipole) has the strongest transport across the equatorial regions (where the differential rotation increases and the field has a maximum), hence redirecting some of the energy budget away from the polar ejecta. The correspondent axisymmetric simulations (dashed curves in Fig. 2) systematically have less energetic ejecta than their 3D counterparts (except for model L1-0 in the first 300 ms p.b.), which combined to the trend of producing faster rotating

https://doi.org/10.1017/S1743921322001193 Published online by Cambridge University Press

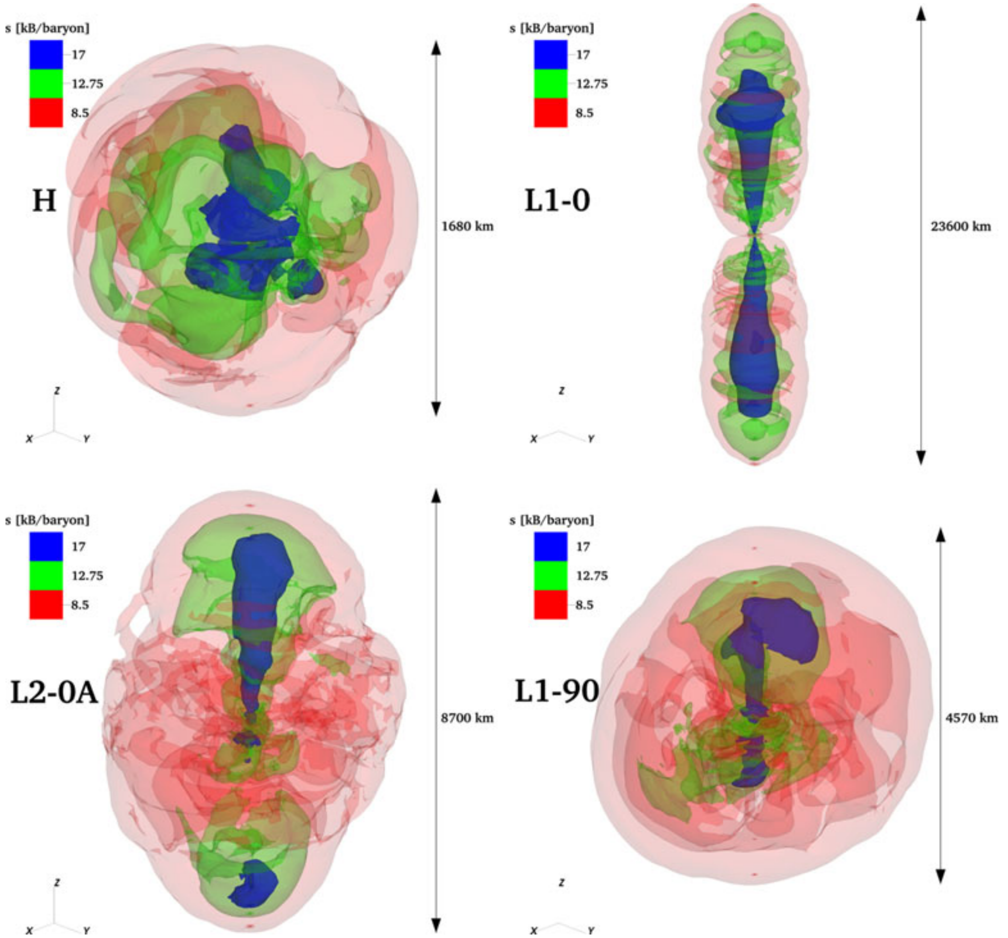

Figure 1. Volume rendering of the specific entropy from four different models at $t = 410$ ms p.b.

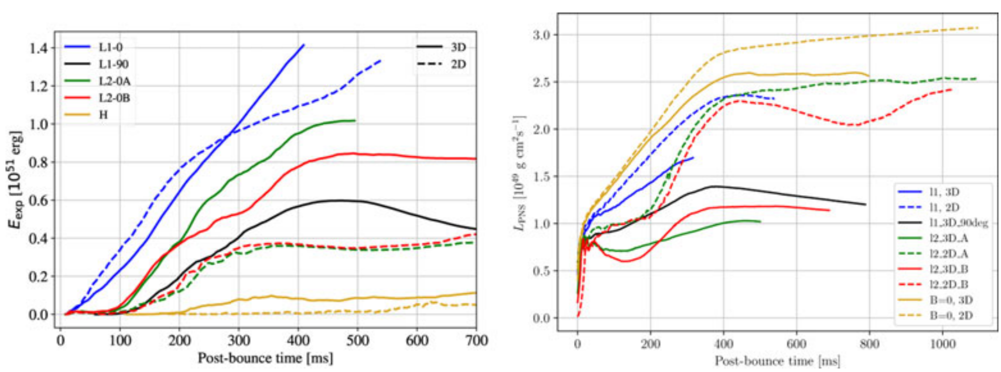

Figure 2. Explosion energy (left panel) and angular momentum of the PNS as a function of post-bounce time for our 3D models (solid lines) and their 2D counterparts (dashed lines).

https://doi.org/10.1017/S1743921322001193 Published online by Cambridge University Press

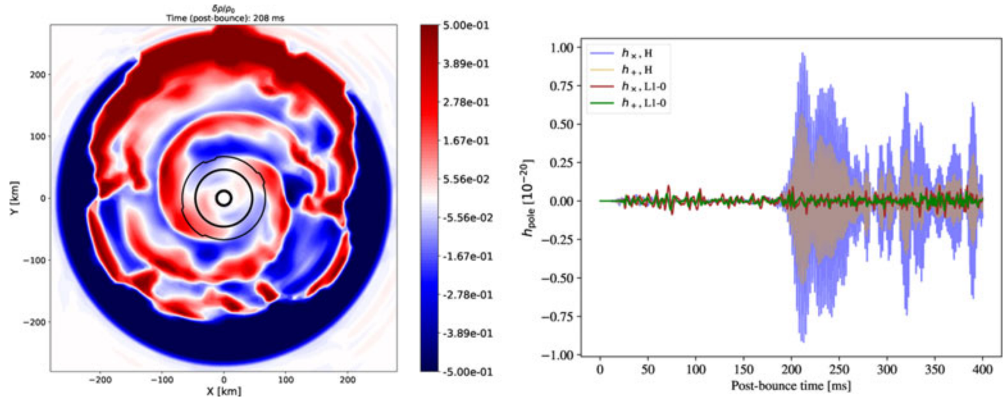

Figure 3. Right panel: non-axisymmetric density distribution in the equatorial plane for model H. Left panel: GW strain over time seen along the rotational axis for models H and L1-0.

PNS shows that 3D models tend to have a higher efficiency with respect to 2D ones in tapping into the rotational energy reservoir to power up the explosion. Moreover, model L2-0A experiences a significant growth of the axisymmetric dipolar component of the magnetic field, which again contributes to an overall more energetic explosion.

Finally, we note a remarkable qualitative difference between all our mangetized simulations and the hydrodynamic one. At about 200 ms p.b. model H shows the onset of the *low* $T/|W|$ *instability* (Takiwaki *et al.* 2021), a corotational instability which manifests itself with large-scale non-axisymmetric spirals in the density distribution within and in proximity of the PNS (right panel of Fig. 3). Such structures are associated with a significant emission of GWs along the poles (left panel), which is however completely absent in model L1-0 (and similarly for all other magnetized simulations). This result suggests that the early transport of angular momentum due to magnetic stresses can efficiently stabilize against the onset of the low $T/|W|$ instability and prevent the otherwise enhanced emission of GWs.

Acknowledgements

MB and JG acknowledge support from the European Research Council (ERC starting grant no. 715368 MagBURST) and from the Très Grand Centre de Calcul du CEA (TGCC) and GENCI for providing computational time on the machines IRENE and OCCIGEN (allocation A0050410317). MO acknowledges support from the Spanish Ministry of Science, Education and Universities (PGC2018-095984-B-I00) and the Valencian Community (PROMETEU/2019/071), the European Research Council under grant EUROPIUM-667912, and from the Deutsche Forschungsgemeinschaft (DFG, German Research Foundation) Projektnummer 279384907 SFB 1245 as well as from the Spanish Ministry of Science via the Ramn y Cajal programme (RYC2018-024938-I).

References

Bugli, M., Guilet, J., Obergaulinger, M., Cerdá-Durán, P. & Aloy, M.A. 2020, *MNRAS*, 492, 58
Bugli, M., Guilet, J. & Obergaulinger, M. 2021, *MNRAS*, 507, 443
Drout M. R., Soderberg A. M., Gal-Yam A. *et al.*, 2011, *ApJ*, 741, 97
Kuroda T., Arcones A., Takiwaki T. & Kotake K. 2020, *ApJ*, 896, 102
Mösta P., Richers S., Ott C. D. et al. 2014, *ApJL*, 785, L29
Nicholl M., Guillochon J. & Berger, E. 2017, *ApJ*, 850, 55
Obergaulinger, M. & Aloy, 2021, *MNRAS*, 503, 4942
Raynaud, R., Guilet, J., Janka, H.T. & Gastine, T. 2020, *Science Advances*, 6(11), 2732

https://doi.org/10.1017/S1743921322001193 Published online by Cambridge University Press

Raynaud, R., Cerda-Duran, P. & Guilet, J., 2022, *MNRAS*, 509, 34103426
Reboul-Salze, A., Guilet, J., Raynaud, R. & Bugli, M. 2021, *MNRAS*, 507, 443
Reboul-Salze, A., Guilet, J., Raynaud, R. & Bugli, M. 2022, sub. to *MNRAS*, arXiv:2111.02148
Takiwaki, T., Kotake, K., & Foglizzo, T. 2021, *MNRAS*, 508, 966
Woosley, S. E. & Heger, A. 2007, *Physics Reports*, 442, 269

https://doi.org/10.1017/S1743921322001193 Published online by Cambridge University Press